

Characterization of Ag-TiO₂ Powders Prepared by Sol-Gel Process

A. EVCIN^{a,*}, E. ARLI^b, Z. BAZ^b, R. ESEN^b AND E.G. SEVER^a

^aAfyon Kocatepe University, Material Science and Engineering Department, Afyonkarahisar, Turkey

^bÇukurova University, Physics Department, Adana, Turkey

In this study, microstructure and electrical properties of Ag-TiO₂ powders, which were prepared by a simple sol-gel method, are investigated. The sol was prepared from titanium iso-propoxide, Ti(OC₃H₇)₄ in iso-propanol (CH₃CHOHCH₃), used as solvent. AgNO₃ was used as the precursor for Ag. For the structural studies, the corresponding gels were allowed to dry naturally for about seven days, dried in an oven at 180 °C for 30 min and then calcined at different temperatures (900, 1000 and 1100 °C). The Ag-TiO₂ nanoparticles were characterized using differential thermal analysis/thermal gravimetry, scanning electron microscopy, energy-dispersive X-ray analysis and X-ray diffraction. The results X-ray diffraction indicate that pure Ag and TiO₂ powders are in rutile phase. However, calcination temperature had not significantly affected the crystalline structure of TiO₂. Scanning electron microscopy images of powders show an aggregation of small spherical particles of dispersed sizes. Annealing of the Ag-TiO₂ sample at high temperature produced more spherical particles, which aggregated to form bigger particles with porous structures. The electrical properties of the samples were measured using HMS-3000 Hall measurement system. The samples were found to be of *n*-type. The conductivity of TiO₂ samples have been explicitly increasing with calcination temperature and with Ag doping.

DOI: [10.12693/APhysPolA.132.608](https://doi.org/10.12693/APhysPolA.132.608)

PACS/topics: 81.20.Fw, 73.63.Bd

1. Introduction

Titanium dioxide (TiO₂) has attracted interest due to such advantages, as effectiveness, chemical stability, non-toxicity, and relatively low cost, strong resistance to the chemical and photo-corrosion, low operational temperature, antibacterial properties and low energy consumption [1–3]. Titanium dioxide is one of the metal oxide semiconductors that have been widely examined for different purposes, since its physical and chemical properties show remarkable changes when the size of the TiO₂ approaches nm scale [4–6]. The modification of TiO₂ by means of metal doping can also affect the properties of TiO₂. Silver, among the other metals, thanks to its high stability and excellent electrical and thermal conductivity, seems to be a favourable titania dopant [7, 8]. In recent years, many researchers have investigated the effect of Ag nanoparticles on properties of TiO₂ [9–15]. Sol-gel is a low temperature, chemical solution method [16–18], which is a proven conventional method for preparation of composite Ag-TiO₂ compound.

In this work, we have prepared nanosized TiO₂ and Ag-TiO₂ powders by sol-gel process, using titanium iso-propoxide and silver nitrate as precursors and iso-propanol as solvent. The effects of Ag on the morphology, crystallization and phase transition of TiO₂ nanoparticles were studied by X-ray diffraction (XRD), scanning electron microscopy (SEM), thermogravimetric analysis (TGA), and differential thermal analysis (DTA) techniques.

2. Materials and methods

To fabricate pure TiO₂ and Ag-TiO₂ powders, titanium iso-propoxide (Ti(OC₃H₇)₄ Aldrich, 98%, molecular weight of 284.22), in iso-propanol ((CH₃)₂CHOH, Sigma-Aldrich, 99.7%, molecular weight 60.10) and silver nitrate (AgNO₃, Sigma-Aldrich, 99%, molecular weight 169.87) were used, as precursor materials.

2.1. Preparation of TiO₂ and Ag-TiO₂ powders

Ti sol and Ag sol were obtained as follows: titanium iso-propoxide was added into isopropanol and silver nitrate was added to deionized water. These solutions were stirred at room temperature for approximately 2 h until they became clear sols. Then they were homogeneously mixed by magnetic stirrer. Then, the formed gel was naturally allowed to dry at room temperature for seven days and dried at 180 °C for 30 min in oven. The obtained powder sample was heated for 4 h in air atmosphere at different temperatures (900, 1000 and 1100 °C), at a heating rate of 10 °C/min. The flow chart, showing the experimental steps to fabricate the samples, is given in Fig. 1.

2.2. Characterization

Thermal analysis of powders was conducted with a Shimadzu TGA/DTA 60H at a heating rate of 20 K/min under nitrogen (99.99% purity) in aluminum pans, in temperature interval of 25 °C to 500 °C. The powdered sample, about 40 mg in weight, was packeted into the aluminum pan, and the gas flow rate was kept at 5 l h⁻¹. DTA/TG diagrams are shown in Fig. 2.

As expected for the Ag-TiO₂ composite powders, the weight losses, associated with the elimination of water

*corresponding author; e-mail: evcin@aku.edu.tr

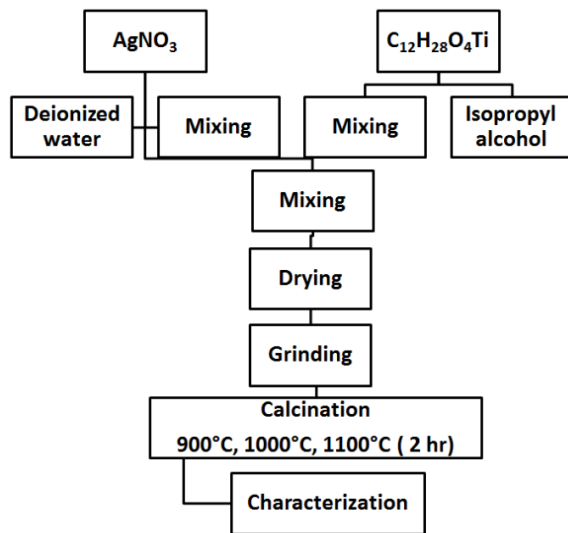
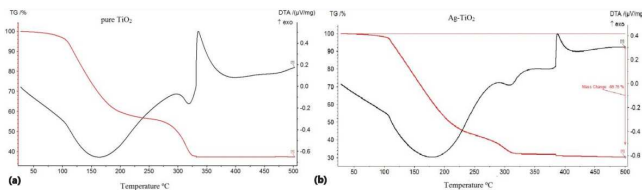


Fig. 1. Experimental flow chart.

Fig. 2. DTA/TG diagrams of pure TiO₂ and Ag-TiO₂ powders.

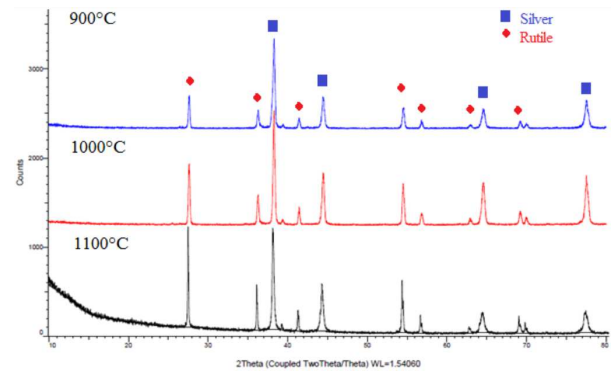
and organic components, are decreased or absent in their TGA thermograms. DTA analysis was performed to determine the effect of silver doping on the crystallization and phase transformation behavior of the TiO₂ nanoparticles.

As can be seen in Fig. 2, the DTA curve revealed an endothermic peak, centered at about 150 °C and three exothermic peaks located at 260, 320 and 365 °C. The endothermic peak was attributed to the elimination of water, adsorbed on the surface of the TiO₂ particles. As can be seen in Fig. 2, for Ag-TiO₂ powder, the anatase-to-rutile phase transformation peak was observed at much lower temperatures. Therefore, the first exothermic peak, observed at about 290 °C can be attributed to the crystallization of amorphous TiO₂ to anatase phase.

The second exothermic peak at 330 °C was associated with the combustion process of the organic species. The third exothermic peak, observed at about 390 °C, was attributed to the phase transformation from anatase to rutile. Similar results have been obtained in the literature [4, 19].

Crystal structures of the powders were characterized via powder X-ray diffraction (XRD, Bruker D 8 Advance) using Cu-K_α X-rays of wavelength $\lambda = 1.5406 \text{ \AA}$ and data were taken in the 2θ range of 20° to 70° with a step of 0.1972°. XRD patterns are shown in Fig. 3.

As can be seen in Fig. 3, peaks corresponding to rutile TiO₂ appear together with the main peaks of silver

Fig. 3. XRD patterns of Ag-TiO₂ powders, thermally treated at different temperatures.

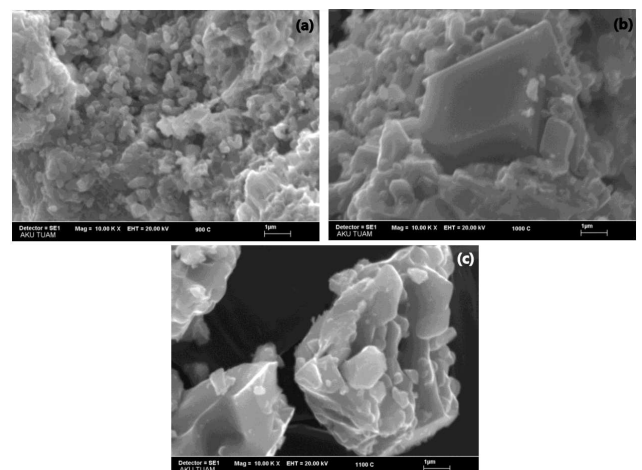
in the XRD pattern of Ag-TiO₂ powders, thermally treated at different temperatures. This indicates that the Ag-TiO₂ powders have crystallized in rutile phase at a temperature over 900 °C. This result matches the literature [4, 10, 11, 13].

The average particle size was calculated by applying the Scherrer equation to the rutile phase (R), for which diffraction peak (the highest intensity peak for pure rutile) appears, as expected, at 2θ of 27° (1 1 0) [20, 21]:

$$D = k\lambda/\beta \cos \theta,$$

where D is the crystal size of the TiO₂, k is a constant (0.89), λ is the X-ray wavelength (1.54 Å), β is the full width at half maximum (FWHM) of the TiO₂ peak and θ is the diffraction angle. The average crystal sizes for Ag-TiO₂ powders, thermally treated at different temperatures, were calculated to be 59, 61 and 84 nm, for the calcination temperature of 900, 1000 and 1100 °C, respectively.

As a complement to this characterization, scanning electron microscopy (SEM, LEO 1430 VP) was utilized, so as to identify the microstructure and morphology of the samples. SEM photos and results of EDX analysis are shown in Figs. 4 and 5, respectively.

Fig. 4. SEM images of Ag-TiO₂ powders, synthesized at different temperatures.

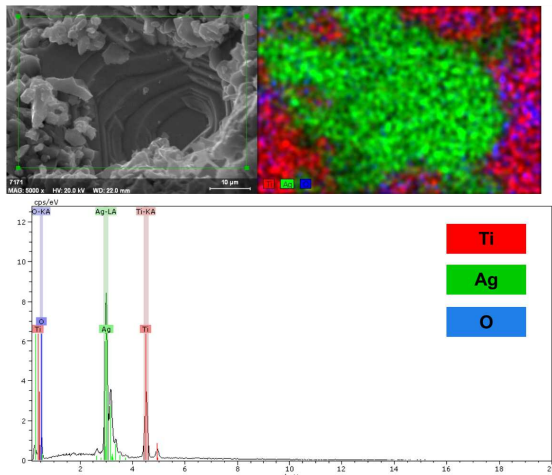


Fig. 5. EDX analysis and elemental mapping of Ag-TiO₂ powder.

Annealing of the Ag-TiO₂ powders at 900 °C has produced more homogeneous spherical particles, which aggregated to form smaller particles with porous structures. Similar morphology is obtained for the Ag-TiO₂ powders, annealed at 1000 °C (Fig. 4), whereas the morphology of the as-prepared Ag-TiO₂ powders annealed at 1000 °C is significantly different [10]. Ag-TiO₂ powders have contained larger aggregated particles. Figure 4 shows a granular structure of average size of approximately between 100 and 400 nm in diameter.

EDX spectra of Ag-TiO₂ powders in Fig. 5 show distribution of Ag, Ti and O components.

The electrical properties of the samples were measured using HMS-3000 Hall measurement system. The Van der Pauw method (linear four point probe) is a technique commonly used to measure the resistivity and the Hall coefficient of a sample. Electrical properties of powders are shown in Table I. This samples were found to be of *n*-type. Sheet and bulk concentrations were found to be of *n*-type [22].

TABLE I

Electrical properties of samples.

	Bulk concentration [1/cm ³]	Mobility [cm ² /Vs]	Resistivity [Ω cm]	Conductivity [1/Ω cm]
900 °C	-1.428×10^{23}	3.838×10^2	1.139×10^{-7}	8.777×10^6
1000 °C	-1.205×10^{23}	5.384×10^2	9.601×10^{-8}	1.042×10^7
1100 °C	-1.928×10^{22}	3.978×10^3	8.14×10^{-8}	1.229×10^7

Annealing of the Ag-TiO₂ samples at high temperature produced spherical particles, which aggregated to form bigger particles with porous structures. However, the mobility slightly increases as the annealing temperature increases. The mobility increase by annealing temperature is due to decrease of carrier scattering on the grain boundaries. Table I shows the mobility, conductivity, resistivity and bulk concentration of the Ag-TiO₂ as functions of the annealing temperature. The resistivity is

inversely proportional to the mobility and the conductivity [23]. The increase of conductivity with working temperature is expected, since number of charge carriers increases with temperature. On the other hand, the increase in the conductivity (decrease of resistivity) with annealing temperatures can be also explained as follows: the grain size increases with annealing temperature, which leads to a decrease in scattering on grain boundaries and hence in resistivity [24].

3. Conclusions

Powders of Ag-TiO₂ have been prepared by the inexpensive sol-gel method. It has been found that while Ag does not enter the TiO₂ lattice, the presence of Ag hinders the anatase grain growth and facilitates the anatase-to-rutile phase transformation.

Ag is present in the Ag⁰ state and the doped silver is highly dispersed and present in Ag form. Ag-TiO₂ powders contain larger aggregated particles and SEM shows a granular structure of average size of approximately between 100 and 400 nm in diameter, for different temperatures.

The powder resistivity and conductivity depend on annealing temperature. The decrease in resistivity allows the correlation between the results obtained by X-ray diffraction and annealing temperature of Ag-TiO₂ powders, synthesized by sol-gel method.

References

- [1] B. Zhao, Y.W. Chen, *J. Phys. Chem. Solids* **72**, 1312 (2011).
- [2] E. Albert, P.A. Albouy, A. Ayril, P. Basa, G. Csik, N. Nagy, S. Roualdes, V. Rouessac, G. Safran, A. Suhajda, Z. Zolnai, Z. Horvölgyi, *RSC Adv.* **5**, 59070 (2015).
- [3] M. Hajivaliei, M. Lashkanpour, *J. Iranian Chem. Res.* **5**, 39 (2012).
- [4] N.Ç. Bezir, A. Evcin, R. Kayali, M.K. Ozen, A. Oktay, *Cryst. Res. Technol.* **51**, 65 (2016).
- [5] B. Otsukarci, Y. Kalpakli, *Acta Phys. Pol. A* **130**, 198 (2016).
- [6] M. Šćepanović, M. Grujić-Brojčinić, M. Mirić, Z. Dohčević-Mitrović, Z. Popović, *Acta Phys. Pol. A* **116**, 603 (2009).
- [7] S. Krejčikova, L. Matejova, K. Koci, L. Obalova, Z. Matej, L. Capekd, O. Solcova, *Appl. Catal. B: Environmental* **111–112**, 119 (2012).
- [8] M. Gorgol, B. Jasińska, R. Reisfeld, V. Levchenko, *Acta Phys. Pol. A* **125**, 778 (2014).
- [9] M. Harikishore, M. Sandhyarani, K. Venkateswarlu, T.A. Nellaippan, N. Rameshbabu, *Procedia Mater. Sci.* **6**, 557 (2014).
- [10] J. García-Serrano, E. Gómez-Hernández, M. Ocampo-Fernández, U. Pal, *Curr. Appl. Phys.* **9**, 1097 (2009).
- [11] J. Yu, J. Xiong, B. Cheng, S. Liu, *Appl. Catal. B: Environmental* **60**, 211 (2005).

- [12] M. Kumar, K.K. Parashar, S.K. Tandi, T. Kumar, D.C. Agarwal, A. Pathak, *J. Spectroscopy* **2013**, 491716 (2013).
- [13] S. Sen, S. Mahanty, S. Roy, O. Heintz, S. Bourgeois, D. Chaumont, *Thin Solid Films* **474**, 245 (2005).
- [14] B. Aysin, A. Ozturk, J. Park, *Ceram. Int.* **39**, 7119 (2013).
- [15] F. Bensouici, T. Souier, A.A. Dakhel, A. Iratni, R. Tala-Ighil, M. Bououdina, *Superlattices Microstruct.* **85**, 255 (2015).
- [16] A. Evcin, D.A. Kaya, *Scientific Res. Essays* **5**, 3682 (2010).
- [17] G. Karwasz, A. Miotello, E. Zomer, R. Brusa, B. Kościelna, C. Armellini, A. Kuzmin, *Acta Phys. Pol. A* **107**, 977 (2005).
- [18] B. Duymaz, Z. Yigit, M. Şeker, F. Dündar, *Acta Phys. Pol. A* **129**, 872 (2016).
- [19] J.Y. Park, I.H. Lee, *J. Nanosc. Nanotechnol.* **10**, 3402 (2010).
- [20] X. Luana, L. Chenb, J. Zhangb, G. Quc, J.C. Flakec, Yi. Wanga, *Electrochim. Acta* **111**, 216 (2013).
- [21] D. Hidalgo, R. Messina, A. Sacco, D. Manfredi, S. Vankova, E. Garrone, G. Saracco, S. Hernandez, *Int. J. Hydrogen Energy* **39**, 21512 (2014).
- [22] W. Liping, L. Baoshun, L. Chao1, Z. Xiujian, *J. Wuhan Univ. Technology – Mater. Sci. Ed.* **24**, 258 (2009).
- [23] H. Han, J.W. Mayer, T.L. Alford, *J. Appl. Phys.* **100**, 083715 (2006).
- [24] K.P. Biju, M.K. Jain, *Thin Solid Films* **516**, 2175 (2008).